Journal of Materials Chemistry C

RSC Publishing

PAPER

View Article Online
View Journal

Cite this: DOI: 10.1039/c3tc31245c

Directly probing the molecular order of conjugated polymer in OPV blends induced by different film thicknesses, substrates and additives†

Joseph Razzell-Hollis,[a] Wing Chung Tsoi[a] and Ji-Seon Kim*[ab]

In organic bulk heterojunction photovoltaic (OPV) devices, formation of a phase-separated morphology of the blend thin film with a high degree of molecular order is required for efficient device performance. Using resonant Raman spectroscopy we monitor *in situ* the P3HT molecular order in P3HT:PCBM blend films influenced by the substrate, film thickness and additives. We report that molecular order depends on substrate for as-cast films, consistent with vertical phase separation driven by a surface energy gradient, but is standardised to a highly ordered state by thermal annealing. *In situ* Raman spectroscopy reveals this phase transition to a more ordered state begins at 40–60 °C for ~120 nm thick blend films, which corresponds to the glass transition temperature (T_g). Ultra-thin (<10 nm thick) blend films had greater P3HT order than the bulk and reorganised at lower temperatures, which we propose is due to a P3HT-rich interfacial layer at the film/air interface, and that extra disordered component retained despite annealing is due to P3HT trapped in a disordered state within the corresponding PCBM-rich substrate interface. Finally we probe how the 1,8-octanedithiol (ODT) additive improves P3HT molecular order in blends by increasing phase separation during deposition, finding that 3% ODT by volume presents a saturation point for improving molecular order, and the improvement is comparable to that by thermal annealing. Through *in situ* experiments and varied fabrication conditions, we have built an understanding of how processing conditions determine conjugated polymer molecular order in blends, with the aim of controlling morphology for higher OPV efficiencies.

Received 29th June 2013
Accepted 10th August 2013

DOI: 10.1039/c3tc31245c

www.rsc.org/MaterialsC

Introduction

Bulk heterojunction thin films comprising of an electron-donating conjugated polymer and an electron-accepting fullerene are generally considered a model material system for organic photovoltaic (OPV) devices, but their power conversion efficiencies are extremely sensitive to the blend film's nanoscale morphology.[1–3] It is understood that OPVs require a large interfacial area between donor and acceptor materials to maximise exciton dissociation, an interpenetrating 3D network for the resulting free charges to reach their respective electrodes, and high molecular order of both component materials for efficient charge transport and longer wavelength absorption.[4–7] Thermal annealing is a common method of improving molecular order of organic semiconductors in blends by increasing phase separation, as blended materials typically experience mutual morphological disruption, which hinders ordering of molecules (crystallisation), but deposition conditions and solvent additives can be used to influence both phase separation and molecular order.[8,9] Here we demonstrate the use of resonant Raman spectroscopy to probe polymer molecular order in blends of poly(3-hexylthiophene) (P3HT) and [6,6]-phenyl-C_{61}-butyric acid methyl ester (PCBM). We investigate the effect of fabrication conditions on the degree of molecular order and vertical phase separation in the blend films, and comment on how those conditions can be used to control morphology for the purposes of increasing device performance.

Raman spectroscopy is a powerful technique that probes the vibrational modes of molecules, providing insight into their chemical structure and molecular conformation.[10,11] The Raman effect can be resonantly enhanced by selecting an excitation wavelength which matches the electronic transition energy of the material. For a conjugated polymer such as P3HT, the main backbone vibrational modes (*e.g.*, symmetric C=C and C–C stretching modes of thiophene rings) are strongly Raman active due to their strong coupling to the π-electrons

[a]*Department of Physics and Centre for Plastic Electronics, Imperial College London, London SW7 2AZ, United Kingdom*

[b]*Department of Materials Science and Engineering, KAIST, Daejeon 305-701, Republic of Korea. E-mail: ji-seon.kim@imperial.ac.uk*

† Electronic supplementary information (ESI) available: Evolution of C=C peak properties during heating for neat P3HT (S1), of the blend under different heating rates (S2) and at different times after each heating step (S3), and the C=C peak properties for neat P3HT films on different substrates (S4); optical microscopy (S5) and AFM surface images (S6) of ODT-treated films, and C=C peak properties of ultra-thin blend films on different substrates (S7). See DOI: 10.1039/c3tc31245c

delocalised along the main backbone, becoming sensitive to conjugation length and thus molecular planarity. Resonant enhancement also permits the selective excitation of ordered (crystalline) and disordered (amorphous) phases of a semiconducting polymer by choosing laser resonance with different phases.[12] It has been found that the main backbone C=C stretch mode of P3HT can be interpreted as a superposition of two peaks representing ordered and disordered phases, represented by semi-crystalline regioregular-P3HT and fully-amorphous regiorandom-P3HT. Therefore, morphological changes that alter molecular order will result in changes to the position and full width half maximum (FWHM) of the C=C Raman peak.[13,14] By comparing the resonant Raman spectra of P3HT:PCBM blends fabricated under different conditions, we monitor changes in P3HT molecular order induced by choice of substrate, blend film thickness, annealing temperature or use of a solvent additive, and so improve our understanding of how blend morphology can be controlled to maximise OPV efficiency for a particular material system.

Results and discussion

Absorption spectra of the thin films provide some indication of molecular order. For neat P3HT, an absorption maximum at ~550 nm and a strong vibronic shoulder at 605 nm (Fig. 1a) indicate the polymer is highly ordered, confirming the semi-crystalline nature of pure P3HT in the thin film.[15] For the as-cast blend film the absorption maximum lies at 495 nm, representing a blue-shift relative to neat P3HT, and the vibronic shoulder at 605 nm is less clearly resolved in the blend. Both of these observations indicate that P3HT molecular order is largely disrupted by the presence of PCBM in the blend film. After thermal annealing the vibronic shoulders become partially restored and the absorption maximum is red-shifted to 510 nm, confirming that thermal annealing increases to some degree polymer molecular order in the blend film.

Raman spectra were measured using 488 nm excitation, which lies within the absorption band of both neat and blended P3HT (see Fig. 1a), in order to achieve resonant enhancement, in particular with more disordered part of the polymers. Fig. 1b shows the Raman spectra of neat P3HT and blended P3HT:PCBM (as-cast and annealed) that are obtained. The Raman spectrum contains two strong vibrational modes associated with the conjugated backbone: the C=C symmetric stretch mode (~1447 cm^{-1}) and the C–C stretch mode (~1380 cm^{-1}) within the thiophene ring. The shapes and intensities of these modes are sensitive to the polymer's molecular order, as is evident from the clear differences between the spectra for neat P3HT and as-cast P3HT:PCBM: neat P3HT has a narrow C=C peak at a Raman shift of 1447 cm^{-1} (FWHM of 28 cm^{-1}) while the as-cast blend has a broader C=C peak at 1458 cm^{-1} (FWHM of 40 cm^{-1}). After thermally annealing the blend, the Raman spectrum closely resembles that of neat P3HT, with a C=C peak at 1449 cm^{-1} (and FWHM of 28 cm^{-1}). The change in P3HT's C=C peak characteristics with molecular order can be understood as a superposition of two components, from ordered P3HT (centred around 1448 cm^{-1}) and disordered P3HT (around 1470 cm^{-1}). The overall degree of molecular order can be described by the position of the peak between these two extremes.[13] Additionally, the peak is widest when there are strong contributions from both ordered and disordered phases, such as in the as-cast blend, with the peak narrowing as the disordered phase is reorganised into a more ordered morphology and the higher-wavenumber contribution reduces, as occurs in thermal annealing. Using this relationship between peak position (and FWHM) and molecular order, we compare different degrees of P3HT molecular order in blend films fabricated under different deposition conditions.

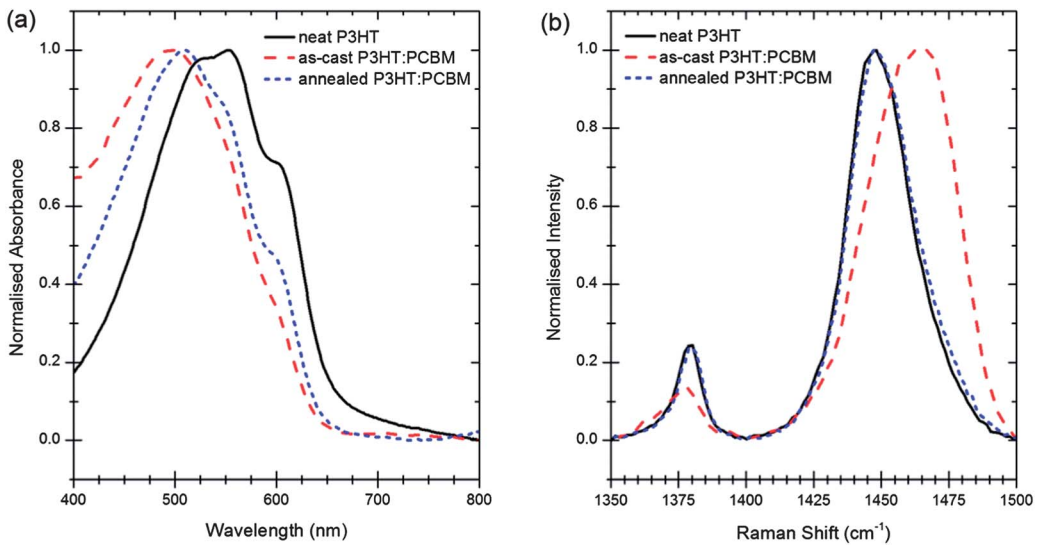

Fig. 1 (a) UV-visible absorption spectra for films of neat P3HT, as-cast P3HT:PCBM and annealed P3HT:PCBM, normalised to the P3HT absorption maximum. (b) Resonant Raman spectra for the same films, normalised to the C=C peak intensity.

Effect of blend film thickness

Variation of molecular order or chemical composition within the blend film can impact on OPV device performance, such as formation of an ultra-thin wetting or capping layer (at the bottom or top interfaces respectively) may act as a barrier to charge extraction if it is rich in the wrong material (*i.e.* hole-transporting P3HT at the electron-extracting electrode).[16] Thin films (100–200 nm) used in OPVs are much thinner than the axial resolution (~μm) of most optical spectroscopy techniques, including resonant Raman, meaning that Raman scattering from interfacial layers (film/substrate or film/air) is dominated by scattering from the bulk of the film. By depositing 'ultra-thin' films that are <10 nm thick, morphology at both air and substrate interfaces can be probed more directly and compared to the bulk morphology (represented by 'thick' films that are ~120 nm). As morphology should be determined during deposition, the air interface can be referred to as such despite measurement under nitrogen.

For as-cast films, the C=C peak of the ultra-thin film is ~1 cm^{-1} lower in Raman shift and ~3 cm^{-1} broader than that of the thick film, due to larger contribution from the lower wavenumber component (see Fig. 2a). The peak shift is comparable to the resolution of the instrument (~1 cm^{-1}) but was reproducible, a shift to lower wavenumbers was observed for all ultra-thin samples examined (see ESI, Fig. S6†). An increased FWHM due to lower wavenumbers confirms a greater fraction of ordered phase is present at the interface than in the bulk. After thermal annealing, the C=C peak from interfacial P3HT is ~8 cm^{-1} wider than that of P3HT in the bulk blend, and greater intensity around 1470 cm^{-1} indicates that the interfacial morphology is less now ordered than the bulk. This suggests that a large fraction of disordered polymer phase is retained despite annealing. We propose that these observations are best explained by describing the ultra-thin film as a vertically-separated bilayer-like structure (see Fig. 2b) made of two interfacial layers rich in either P3HT or PCBM, where a P3HT-rich layer with reduced disruption of polymer packing by PCBM results in greater overall molecular order prior to annealing, and a corresponding PCBM-rich layer that contains some P3HT polymer dissolved in a highly disordered amorphous phase (due to the density of surrounding PCBM molecules) that is not altered by annealing. Whether these interfacial layers hinder charge extraction and overall device performance depends on which material is concentrated at which interface.

In situ Raman spectroscopy

Using *in situ* resonant Raman spectroscopy, we investigated temperature-induced molecular reorganisation within the blend film in order to infer the direction of vertical phase separation. A film of neat P3HT showed little change in Raman spectrum during *in situ* heating to 150 °C or subsequent cooling (not shown, see ESI, Fig. S1†) but for the blend film a distinctive phase transition was observed during heating. Once heated above ~50 °C there was a reduction of the disordered component of P3HT's C=C peak relative to the ordered component (see Fig. 3a), which was not reversed upon cooling back to room temperature (Fig. 3b). The transition was found to be independent of the heating profile used, with similar peak positions and peak widths measured at a given temperature for samples heated at different rates or held for different durations after each step (see ESI, Fig. S2 and S3†). In terms of C=C peak position, a sharp transition was observed for the 'thick' film (Fig. 3c), beginning at ~50 °C and completing by 90 °C, for the ultra-thin film it began at a lower temperature, ~30 °C, and was

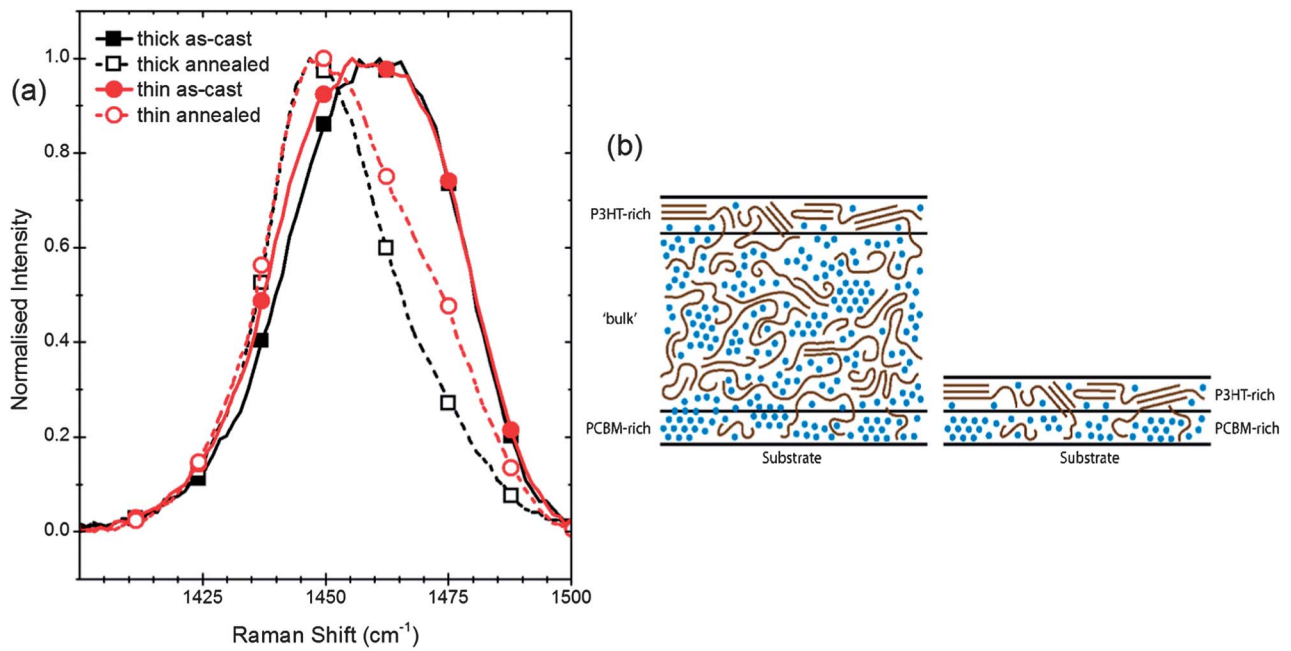

Fig. 2 (a) Resonant Raman spectra for thick (~120 nm) and ultra-thin (<10 nm) P3HT:PCBM films deposited on ITO, before and after annealing. (b) Diagram of proposed vertical structure within thick and ultra-thin P3HT:PCBM films, showing interfacial layers rich in either P3HT or PCBM.

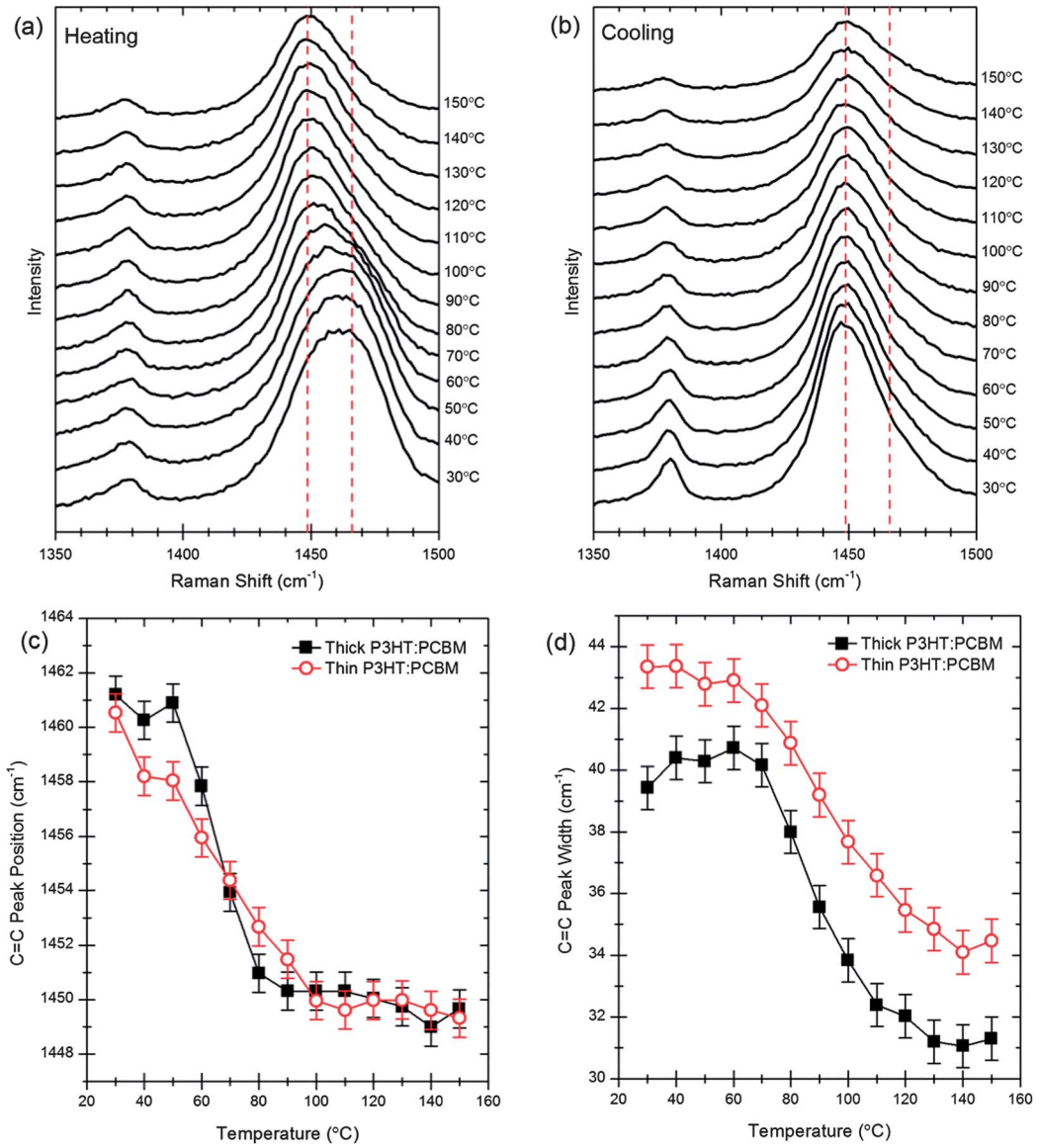

Fig. 3 *In situ* resonant Raman spectra for a 120 nm thick P3HT:PCBM film on ITO/PEDOT:PSS, during stepped heating (a) and cooling (b) processes. Spectra are offset for clarity. Evolution of C=C peak position (c) and FWHM (d) during stepped heating.

more gradual, completing by 110 °C. Reduction of FWHM, due to reduced contribution from the disordered phase, occurred at slightly higher temperatures and was more gradual for the thinner film (Fig. 3d). We interpret this phase transition, which clearly represents an increase in molecular order within the film, as the reorganisation of disordered P3HT into the ordered form once heated above a critical temperature: the glass transition temperature (T_g) of the blend. For the thick film, we estimate a T_g of ~50 °C, which agrees well with reported values for 1 : 1 P3HT:PCBM blends as measured by DSC and ellipsometry.[17,18] *In situ* studies of device performance during thermal annealing have also shown that the increase in short-circuit current (J_{SC}) begins at roughly the same temperature, that we can ascribe to improving charge transport due to higher molecular order of polymer.[18,19] The temperature at which P3HT molecular order is maximised, ~130 °C, should indicate the minimum temperature of annealing required to achieve proper phase separation between P3HT and PCBM into domains of high polymer molecular order.

For the ultra-thin film, the phase transition begins at a lower temperature, with the C=C peak shifting to lower wavenumbers from the onset of the experiment (30 °C). Roth *et al.* have described reduction of T_g with decreasing film thickness as a consequence of higher molecular mobility at the unconfined air interface and weak polymer–substrate interactions.[20] We consider the same explanation applies to polymer:fullerene blend films, with the lower-temperature reorganisation evident of a P3HT-rich film/air interface that requires less thermal energy to rearrange into a highly ordered state. The more gradual change in both peak position and FWHM for the ultra-thin film can be described as a consequence of the corresponding PCBM-rich film/substrate layer containing some

molecules of P3HT that require greater thermal energy to reorganise (due to disruption by surrounding PCBM) compared to polymers in the bulk blend. The existence of a P3HT-rich air interface and PCBM-rich substrate interface (shown in Fig. 2b) in the active layer will have important implications for electrical properties in standard (non-inverted) device architectures, as the low concentration of P3HT at the substrate interface (near the ITO electrode) will present a barrier to hole extraction, while the low concentration of PCBM near the air interface will hinder electron extraction.

Effect of substrate

In OPV devices the active layer is usually deposited onto the transparent electrode, Indium Tin Oxide (ITO), often with an interlayer of organic polymer such as PEDOT:PSS to improve charge extraction. For the investigation into how molecular order of the active blend material is influenced by the substrate, we also deposited P3HT:PCBM onto substrates of plain Quartz (Q) and Quartz with a PEDOT:PSS interlayer. Fig. 4a shows that the C=C peaks for as-cast films deposited on the different substrates were broad (~40 cm^{-1}) and at high wavenumbers (1458–1464 cm^{-1}), typical of a fairly disordered morphology. There was a ~6 cm^{-1} variation in C=C peak position between the as-cast P3HT:PCBM films on different substrates that was not observed in neat P3HT films (see ESI, Fig. S4†), revealing that the molecular order of the as-cast blend depends in part on the substrate it is deposited on. We found that the most ordered as-cast film is on ITO (1458 cm^{-1}) and the most disordered film is on Quartz/PEDOT:PSS (1464 cm^{-1}), and that the inclusion of a PEDOT:PSS interlayer increases disorder, shifting the C=C peak to higher wavenumbers by 2.9 cm^{-1} on ITO and 1.2 cm^{-1} on Quartz. These shifts were small enough to be comparable to instrumental resolution, but the trend was reproducible: inclusion of the PEDOT:PSS interlayer produces a similar shift for ultra-thin films (see ESI, Fig. S6†). We propose to explain this

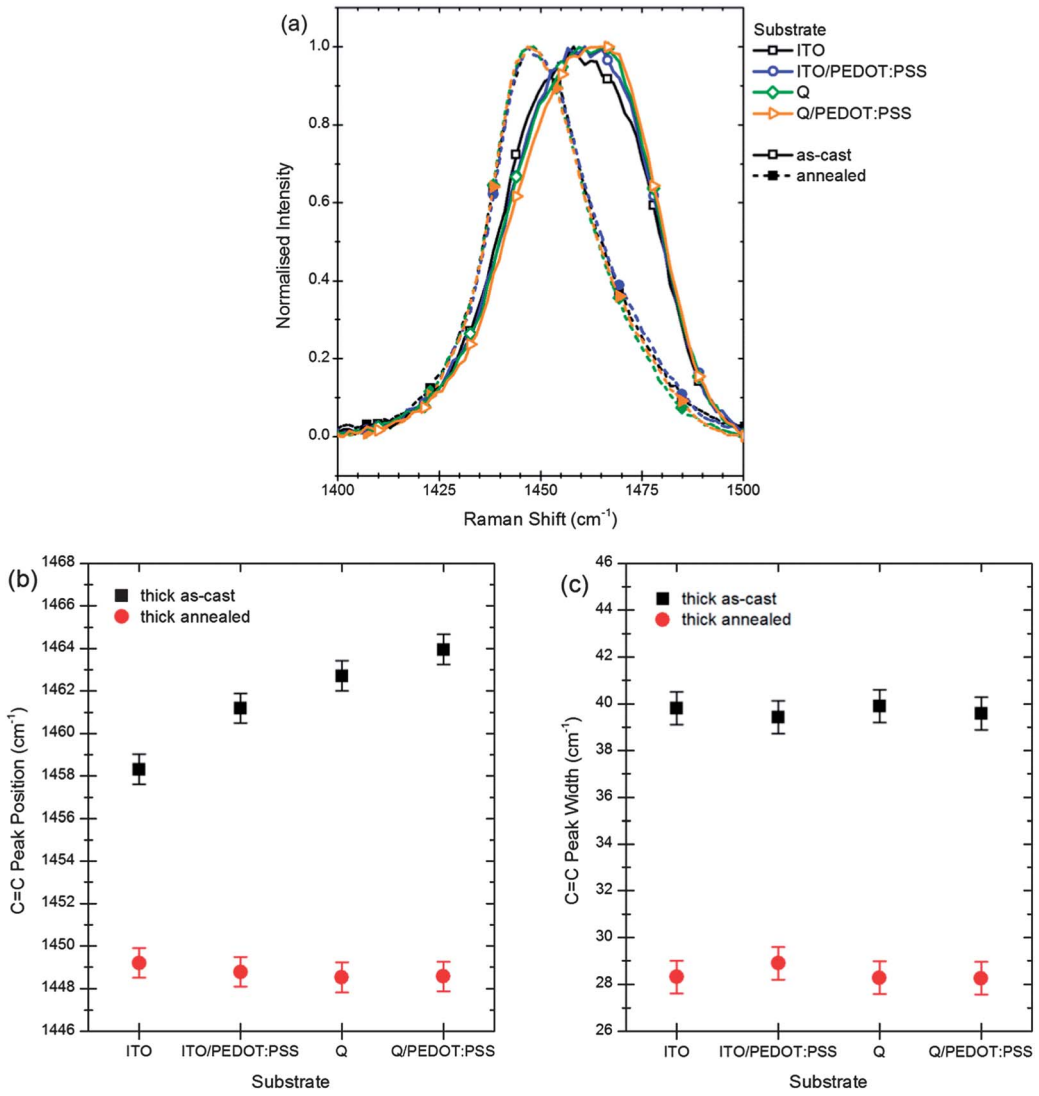

Fig. 4 Normalised resonant Raman spectra (a), C=C peak positions (b) and FWHM (c) for as-cast (solid lines) and annealed (dashed lines) films of P3HT:PCBM deposited on four different substrates: ITO and Quartz (Q), with and without a PEDOT:PSS interlayer.

substrate-dependent variation in molecular order as a consequence of vertical phase separation, where greater separation between the two components means a less intimately mixed morphology and thus reduced disruption of P3HT molecular order by interactions with PCBM molecules. The driving force behind vertical phase separation is the difference in surface energy between substrate and air interfaces,[8,21] which acts on P3HT and PCBM (which have reported surface energies of 27.2 and 38.2 mJ m^{-2} respectively) during deposition to create gradients in chemical composition through the thickness of the active layer. Therefore our observation that as-cast molecular order is reduced by the inclusion of a PEDOT:PSS interlayer is consistent with work by Campoy-Quiles *et al.*, who reported that P3HT:PCBM films on PEDOT:PSS showed less vertical phase separation than the same films on Quartz.[8] Differences in lateral phase separation can be dismissed as there was no variation between optical microscopy images taken of the different samples under 50× magnification (see ESI, Fig. S5†).

The P3HT- and PCBM-rich interfacial layers described previously agree with the direction of vertical phase separation predicted by their surface energies: lower-surface energy P3HT collects at the low-surface energy air interface and higher-surface energy PCBM at the high-surface energy substrate interface. The bulk of the film is not morphologically homogenous but a continuum of domains with different degrees of molecular order depending on the local chemical composition, with the greatest overall molecular order achieved on the highest energy substrate, plasma-treated ITO (which has a reported surface energy of ~65 mJ m^{-2}).[22]

After thermal annealing, the C=C peaks were narrow (FWHM of ~28 cm^{-1}) and shifted to lower wavenumbers (~1449 cm^{-1}), with variation in C=C peak position between films on different substrates reduced to only ~1 cm^{-1}, indicating that the highly-ordered annealed state of P3HT is independent of substrate. We conclude that annealing acts to standardise morphology to a thermodynamically favourable state of significant phase separation and high polymer molecular order, and thus the substrate's influence on P3HT molecular order is a purely kinetic effect imposed only during deposition.

Upon heating the films on different substrates to 150 °C (Fig. 5), the C=C peaks move to lower wavenumbers and smaller FWHM as expected. The temperature range of the phase transition varied between substrates: the change in C=C peak position occurred between 40 and 80 °C on ITO, and between 60 and 100 °C on Q/PEDOT:PSS (there was less variation in the temperature range for changes in FWHM). T_g appears to correlate to the initial degree of molecular order present, with the most ordered as-cast film (on ITO) having the lowest onset temperature for the phase transition. This agrees with our understanding that the most-ordered as-cast film has the greatest vertical phase separation, and are less intermixed with PCBM, resulting in a T_g that is closer to that of pristine P3HT (literature values of 12–20 °C).[17,18] In conclusion, P3HT molecular order in P3HT:PCBM blend films is strongly influenced by substrate during deposition, possibly through the formation of a vertically phase-separated morphology driven by substrate surface energy, but after thermal annealing the morphology is standardised to a highly ordered state with significant phase separation that is independent of substrate.

Effect of additives

Chemical additives have already been investigated as a method of achieving higher performance OPV devices by encouraging phase separation during deposition, and so eliminating the need for a subsequent thermal annealing step.[9,23,24] High boiling point additives such as 1,8-octanedithiol (ODT) act as a good solvent for PCBM and a poor solvent for P3HT, resulting in segregation during deposition to form an as-cast blend of purer domains with a high degree of molecular order. Chen *et al.* found that the optimum concentration of ODT for improving

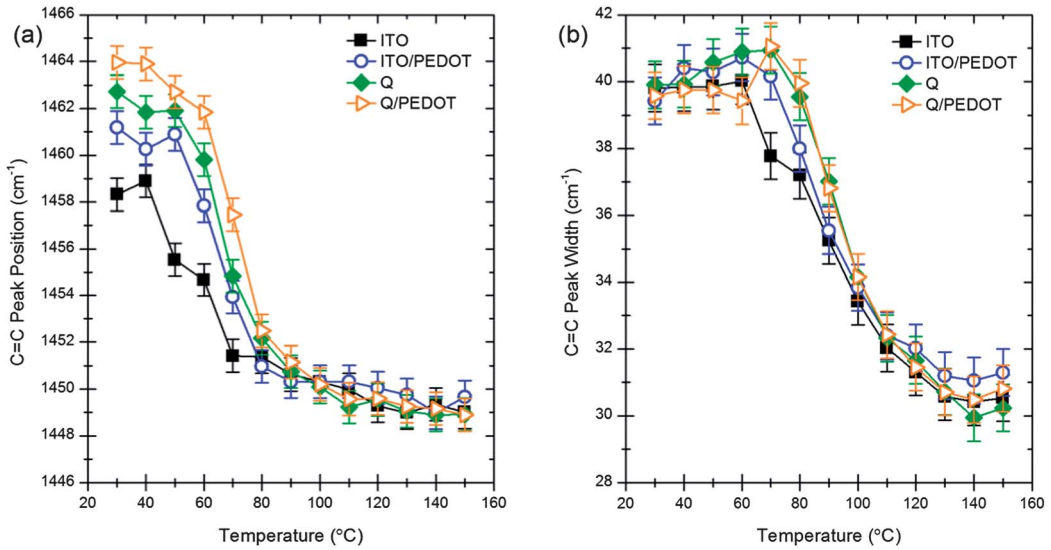

Fig. 5 Evolution of C=C peak position (a) and FWHM (b) during stepped heating for films of P3HT:PCBM deposited on four different substrates: ITO and Quartz (Q), with and without a PEDOT:PSS interlayer.

as-cast device efficiency was 3% by volume, due to a greater short-circuit current and fill factor.[24] Using resonant Raman and optical absorption spectroscopy, we demonstrate how molecular order of the as-cast blend film varies with ODT concentrations between 0 and 9% by volume in order to better explain the effect of ODT on device performance. The effect of ODT on ultra-thin films was not examined as part of this work, but will form part of future work on the morphological effects of additives.

As shown in Fig. 6a, the C=C peak of P3HT in the blend is narrowed and shifted to lower wavenumbers by the introduction of ODT to the spin-coating solution, consistent with increased as-cast molecular order with greater ODT concentration (no additive peaks were observed between 500 cm^{-1} and 1900 cm^{-1}, thus any contribution to the Raman spectrum by scattering from non-resonant ODT can be treated as negligible compared to resonant scattering from P3HT). Fig. 6c reveals that with 1% ODT by volume the resulting C=C peak was shifted to ~1448 cm^{-1} (FWHM of ~31 cm^{-1}), comparable to that of a thermally annealed film (~1449 cm^{-1}, FWHM of ~28 cm^{-1}), indicating that a similar improvement in molecular order has been achieved by the ODT treatment. Higher ODT concentrations further improved molecular order of the blended P3HT, 3% ODT resulted in a similar peak position (~1448 cm^{-1}) and a reduced FWHM (~28 cm^{-1}). No further shift to lower wavenumbers or narrower FWHM was seen when 9% ODT was used, suggesting that 3% ODT represents a saturation point for the maximisation of as-cast molecular order.

To better understand the effect of ODT on the phase separation of the blend, AFM was used to measure surface roughness for each film (which is qualitatively related to the domain size and phase separation of the two materials). Fig. 6b shows that ODT-treated films were rougher (more phase separated) than the untreated film, following an approximately linear trend with concentration. With 3% ODT, surface roughness significantly exceeded that produced by thermal annealing (10.6 nm *vs.*

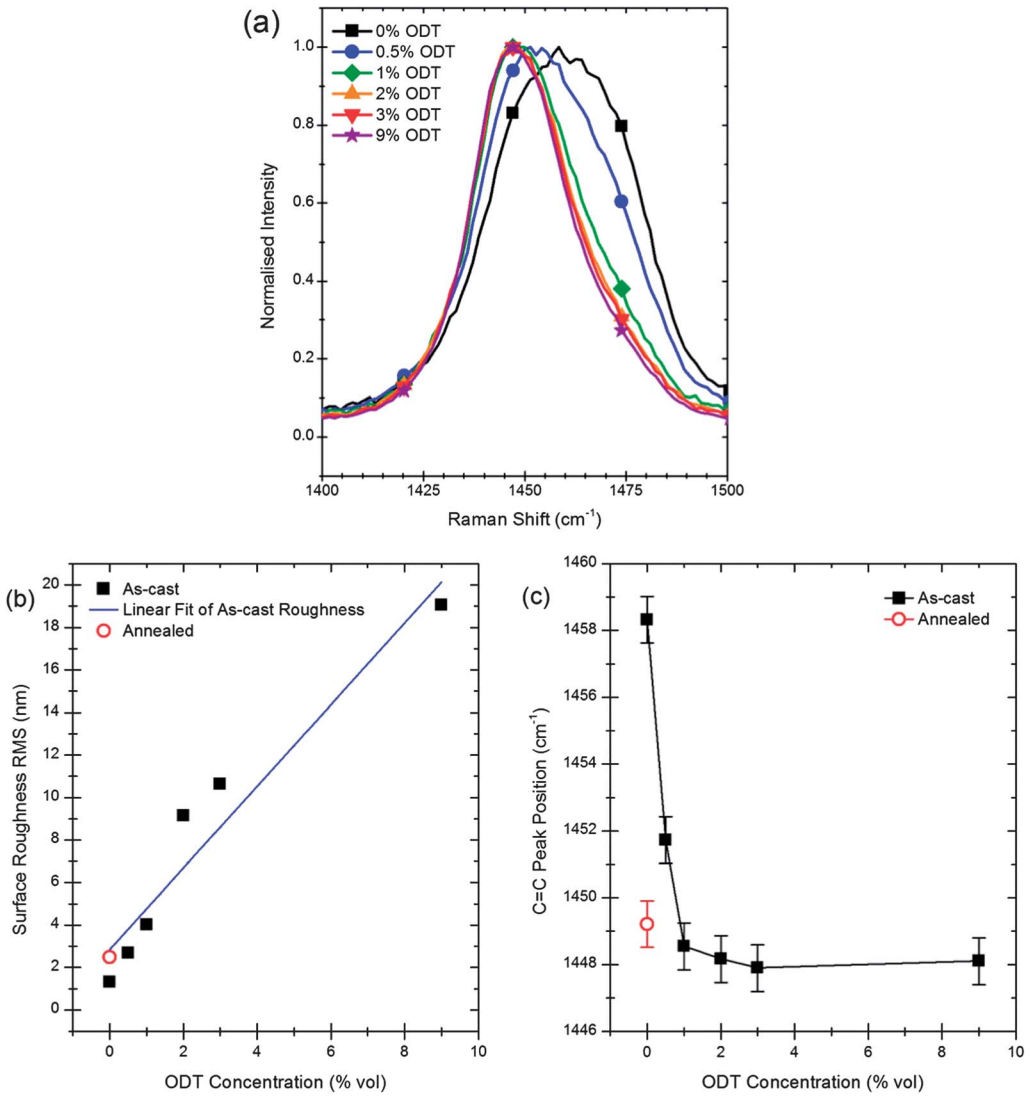

Fig. 6 (a) Raman spectra for P3HT:PCBM films spin-coated from solutions containing different concentrations of ODT. (b) Surface roughness, as measured by AFM, for the same films, with annealed film without ODT shown for comparison. (c) C=C peak positions for the same films.

2.4 nm respectively), suggesting a highly phase-separated blend has been deposited with correspondingly high molecular order. For 3% and 9% ODT the phase separation was sufficiently large that it was observable through an optical microscope with 50× magnification (images shown in ESI, Fig. S5†), and much larger with 9% ODT than 3%. This confirms that ODT acts to increase molecular order by increasing separation of the two materials (polymer and fullerene) into different phases during deposition, producing larger pure domains with greater crystallinity. This improvement in molecular order and crystallinity explains the greater short-circuit current and device efficiency reported in the literature for ODT-treated films, but excessive phase separation into domains much larger than the exciton diffusion length will limit exciton dissociation and reduce device efficiency. Consequently, the concentration that produces the smallest phase separation necessary to maximise molecular order (*i.e.* the observed saturation point at 3% by volume) represents the optimal concentration for improving device performance. The comparable improvement of molecular order obtained by ODT-treatment and thermal annealing reinforces the claim that solution-based processes could be used in future to improve device performance without the need for costly post-treatment steps. The effect of the additive ODT on phase separation during deposition, based on differences in solubility, means that it can be used for other polymers that suffer from reduced molecular order when blended with fullerene.

Experimental section

P3HT:PCBM films were deposited from a solution of regioregular-P3HT (Merck) and PCBM (Solenne b.v) in chlorobenzene at two different concentrations: thick (∼120 nm) films were made using a 40 mg mL^{-1} (total concentration) solution spin-coated at 2000 rpm for 120 seconds, ultra-thin (6 ± 1.4 nm) films were made using a 5 mg mL^{-1} solution spin-coated at 5000 rpm for 120 seconds. The substrates were ITO coated on glass (Psiotec Ltd) and fused Quartz (Spectrosil, UQG Ltd), cleaned by ultrasonication and baked at 150 °C for 30 min, then treated with 3 minutes of O_2 plasma-ashing at 80 W prior to deposition of the organic layers. For 'ITO/PEDOT:PSS' and 'Q/PEDOT:PSS' substrates, a ∼40 nm thick interlayer of poly(3,4-ethylenedioxythiophene):poly(styrenesulfonate) (PEDOT:PSS) purchased from Heraeus was spin-coated onto cleaned ITO and Quartz at 4000 rpm for 90 seconds, and baked at 150 °C for 30 minutes before deposition of the P3HT:PCBM layer. Thicknesses were measured using a Dektak profilometer. For additive-treated blends samples, 1,8-octanedithiol (Sigma-Aldrich) was added to standard solutions of P3HT:PCBM in chlorobenzene (1 : 1 by weight, totalling 40 mg mL^{-1}) to make up concentrations of 0.5, 1, 2, 3 and 9% ODT by volume and then spin-coated onto plasma-treated ITO at 2000 rpm for 120 seconds.

UV-vis absorption spectra were obtained using a Shimadzu UV-2550 spectrophotometer with Quartz and ITO references. AFM measurements were performed on an NT-MDT NanoScope, using TiN tips (NT-MDT, 1.45–15.1 N m^{-1}) in tapping mode with a scan area of 2.5 × 2.5 μm. Surface roughnesses were calculated using the Gwyddion software package.

Raman spectra were obtained using a Renishaw inVia Raman microscope with a 50× objective in a backscattering configuration, and a Linkam thermal stage as the inert sample chamber. For resonance excitation for P3HT, the excitation source was a 488 nm (Ar ion) laser. To reduce photo-degradation of the sample, the sample chamber was purged with N_2 gas and the laser-spot was defocused to ∼8 μm. Laser power was ∼0.09 mW for thick films and ∼0.9 mW for thin films, with acquisition times of 12 s and 18 s respectively. For the *in situ* annealing, samples were heated from 30 °C to 150 °C, annealed at 150 °C for 30 minutes and then cooled back to 30 °C. Heating/cooling was carried out in 10 °C steps at 10 °C min^{-1}, with spectra recorded after each 10 °C step and every 10 minutes during annealing.

Conclusions

The resonant Raman spectrum of the polymer P3HT was used to probe its molecular order, and build a detailed model of the morphology that forms when P3HT is blended with PCBM according to the relationship between intermixing of the two materials and disruption of P3HT molecular order. This morphology is determined by vertical phase separation during deposition and molecular reorganisation during thermal annealing. Interfacial molecular order was studied using ultra-thin films and *in situ* thermal annealing, revealing the presence of a more ordered P3HT-rich interfacial layer that has a lower glass transition temperature than the bulk blend, placing it at the unconfined air interface. This and the corresponding PCBM-rich substrate interface (containing some highly disordered P3HT) will hinder effective charge extraction towards electrodes in non-inverted devices. The vertical phase separation that exists between these interfacial layers in thicker as-cast films was found to depend on the substrate for as-cast films, but that thermal annealing at 150 °C standardises the morphology to a more phase-separated highly-ordered state independent of substrate. The vertical phase separation is driven by the surface energy of the substrate, with plasma-treated ITO achieving the highest molecular order and inclusion of a PEDOT:PSS interlayer reducing it. During *in situ* heating, a phase transition towards higher P3HT molecular order was observed for the thick blend films, with an onset temperature of ∼50 °C that is consistent with the blend's glass transition temperature. We demonstrate that the additive ODT improves P3HT molecular order produced during deposition, reaching a saturation point at a concentration of 3% by volume at which P3HT and PCBM are effectively separated at the micro-scale, which agrees with the optimisation of device properties in the literature. The molecular order obtained is comparable to that achieved by annealing, reinforcing the claim that additives could be used to eliminate annealing steps from large-scale fabrication without compromising on efficiency.

We have demonstrated that resonant Raman spectroscopy not only probes molecular order of a semiconducting polymer but also provides information on the complex relationship between fabrication conditions, blend morphology and device performance in OPVs made from organic blends. With *in situ*

monitoring of molecular order, important morphological information is revealed and it becomes possible to study the kinetics of thermal reorganisation that are critical to thermal treatment and stability. The flexibility of the technique to sample conditions also offers the possibility of future investigations of morphology within complete devices, for *in situ* monitoring and correlation of morphological properties to device properties.

Acknowledgements

This work was funded by the EPSRC through the Plastic Electronics Doctoral Training Centre (EP/G037515/1), the Scalable Low Cost Organic Photovoltaic Solar Cells (SCALLOPS) Project (TP no. 100897) and by the World Class University (WCU) program (Grant no. R32-10051) in Korea.

Notes and references

1 H. Hoppe, M. Niggemann, C. Winder, J. Kraut, R. Hiesgen, A. Hinsch, D. Meissner and N. S. Sariciftci, *Adv. Funct. Mater.*, 2004, **14**, 1005–1011.
2 H. Hoppe, T. Glatzel, M. Niggemann, A. Hinsch, M. C. Lux-Steiner and N. S. Sariciftci, *Nano Lett.*, 2005, **5**, 269–274.
3 X. Yang and J. Loos, *Macromolecules*, 2007, **40**, 1353–1362.
4 M. Reyes-Reyes, K. Kim and D. L. Carroll, *Appl. Phys. Lett.*, 2005, **87**, 083506.
5 M. Al-Ibrahim, O. Ambacher, S. Sensfuss and G. Gobsch, *Appl. Phys. Lett.*, 2005, **86**, 201120.
6 H. Hoppe and N. S. Sariciftci, *J. Mater. Chem.*, 2006, **16**, 45.
7 G. Dennler, M. C. Scharber and C. J. Brabec, *Adv. Mater.*, 2009, **21**, 1323–1338.
8 M. Campoy-Quiles, T. Ferenczi, T. Agostinelli, P. G. Etchegoin, Y. Kim, T. D. Anthopoulos, P. N. Stavrinou, D. D. C. Bradley and J. Nelson, *Nat. Mater.*, 2008, **7**, 158–164.
9 A. Pivrikas, H. Neugebauer and N. S. Sariciftci, *Sol. Energy*, 2011, **85**, 1226–1237.
10 J.-S. Kim, P. K. H. Ho, C. E. Murphy, N. Baynes and R. H. Friend, *Adv. Mater.*, 2002, **14**, 206–209.
11 H. Liem, P. Etchegoin, K. S. Whitehead and D. D. C. Bradley, *J. Appl. Phys.*, 2002, **92**, 1154.
12 M. L. Shand, R. R. Chance, M. LePestollic and M. Schott, *Phys. Rev. B: Condens. Matter Mater. Phys.*, 1982, **25**, 4431–4436.
13 W. C. Tsoi, D. T. James, J. S. Kim, P. G. Nicholson, C. E. Murphy, D. D. C. Bradley, J. Nelson and J.-S. Kim, *J. Am. Chem. Soc.*, 2011, **133**, 9834–9843.
14 Y. Gao and J. K. Grey, *J. Am. Chem. Soc.*, 2009, **131**, 9654–9662.
15 Y. Gao, T. P. Martin, E. T. Niles, A. J. Wise, A. K. Thomas and J. K. Grey, *J. Phys. Chem. C*, 2010, **114**, 15121–15128.
16 M. Chiesa, L. Bu, J. S. Kim, R. Shikler, R. H. Friend and H. Sirringhaus, *Nano Lett.*, 2005, **5**, 559–563.
17 J. Zhao, A. Swinnen, G. Van Assche, J. Manca, D. Vanderzande and B. Van Mele, *J. Phys. Chem. B*, 2009, **113**, 1587–1591.
18 A. J. Pearson, T. Wang, R. A. L. Jones, D. G. Lidzey, P. A. Staniec, P. E. Hopkinson and A. M. Donald, *Macromolecules*, 2012, **45**, 1499–1508.
19 N. D. Treat, C. G. Shuttle, M. F. Toney, C. J. Hawker and M. L. Chabinyc, *J. Mater. Chem.*, 2011, **21**, 15224.
20 C. B. Roth and J. R. Dutcher, *J. Electroanal. Chem.*, 2005, **584**, 13–22.
21 P. G. Karagiannidis, D. Georgiou, C. Pitsalidis, A. Laskarakis and S. Logothetidis, *Mater. Chem. Phys.*, 2011, **129**, 1207–1213.
22 J. S. Kim, R. H. Friend and F. Cacialli, *J. Appl. Phys.*, 1999, **86**, 2774.
23 J. Peet, J. Y. Kim, N. E. Coates, W. L. Ma, D. Moses, a. J. Heeger and G. C. Bazan, *Nat. Mater.*, 2007, **6**, 497–500.
24 H.-Y. Chen, H. Yang, G. Yang, S. Sista, R. Zadoyan, G. Li and Y. Yang, *J. Phys. Chem. C*, 2009, **113**, 7946–7953.